Prevention of dietary fat-fueled ketogenesis attenuates BRAF V600E tumor growth
Xia, et al.

SUPPLEMENTAL INFORMATION

SUPPLEMENTAL FIGURES

Figure S1 related to Figure 1

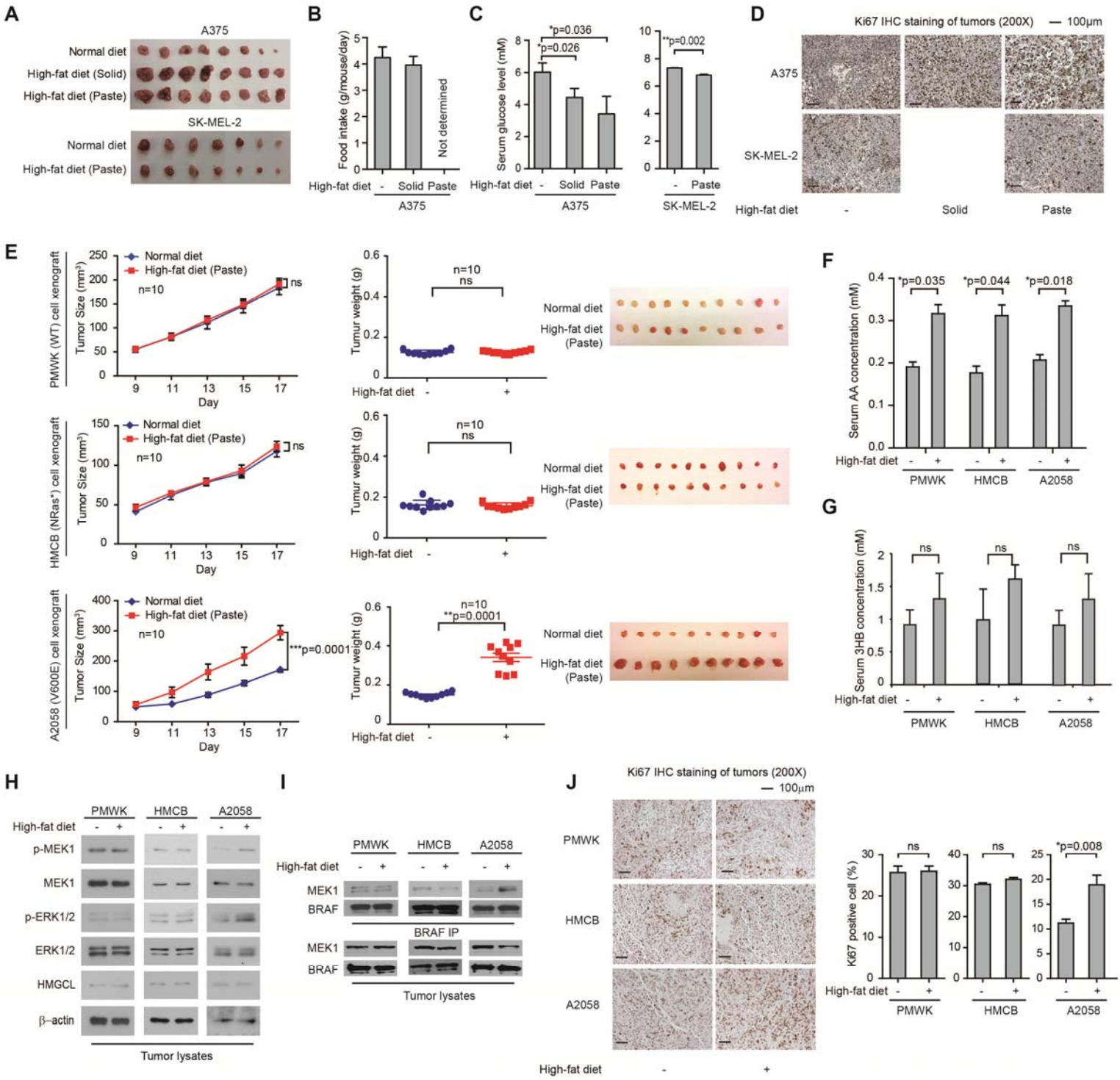

Figure S1. High-fat diet selectively promotes tumor growth potential of BRAF V600E-positive melanoma cells in xenograft nude mice. Related to Figure 1

(A) Xenograft tumor size in nude mice inoculated with human melanoma BRAF V600E-positive A375 (*upper*) or SK-MEL-2 (NRAS Q61R; *lower*) cells and fed with normal diet, or different high-fat diets.
(B-C) Food intake monitoring (B) and serum glucose level (C) of xenograft nude mice.
(D) Representative images of IHC staining of Ki67 (brown color) in tumor tissue samples from xenograft mice treated with normal or different high-fat diets. Scale bars represent 100 μM.
(E) Xenograft tumor growth (*left* panels), weight (*middle* panels) and size (*right* panels) in nude mice inoculated with human melanoma PMWK (BRAF WT, *upper*), HMCB (NRAS Q61K, *middle*), or BRAF V600E-positive A2058 (*lower*) cells and fed with normal or high-fat diets. Data are mean ± SEM for tumor growth and mean ± s.d. for tumor weight; p values were obtained by a two-way ANOVA test for tumor growth rates and a two-tailed Student's *t* test for tumor masses.
(F-G) AA (F) and 3HB (G) levels in serum harvested from PMWK, HMCB, and A2058 xenograft mice fed with normal or high-fat diets. Data are mean ± s.d.; n=3; p values were obtained by a two-tailed Student's *t* test.
(H-I) Western blot results show MEK1 and ERK1/2 phosphorylation (H) and BRAF-MEK1 binding (I) in tumor tissue samples obtained from PMWK, HMCB, and A2058 xenograft mice fed with normal or high-fat diets.
(J) Summarized results of immunohistochemical (IHC) staining assay. Representative images of IHC staining of Ki67 (brown color, *left*) and detection of Ki67-positive cells in tumor tissue samples (*right*) from PMWK, HMCB, and A2058 xenograft mice fed with normal or high-fat diet. Data are mean ± s.d.; p values were obtained by a two-tailed Student's *t* test.

Figure S2 related to Figure 2

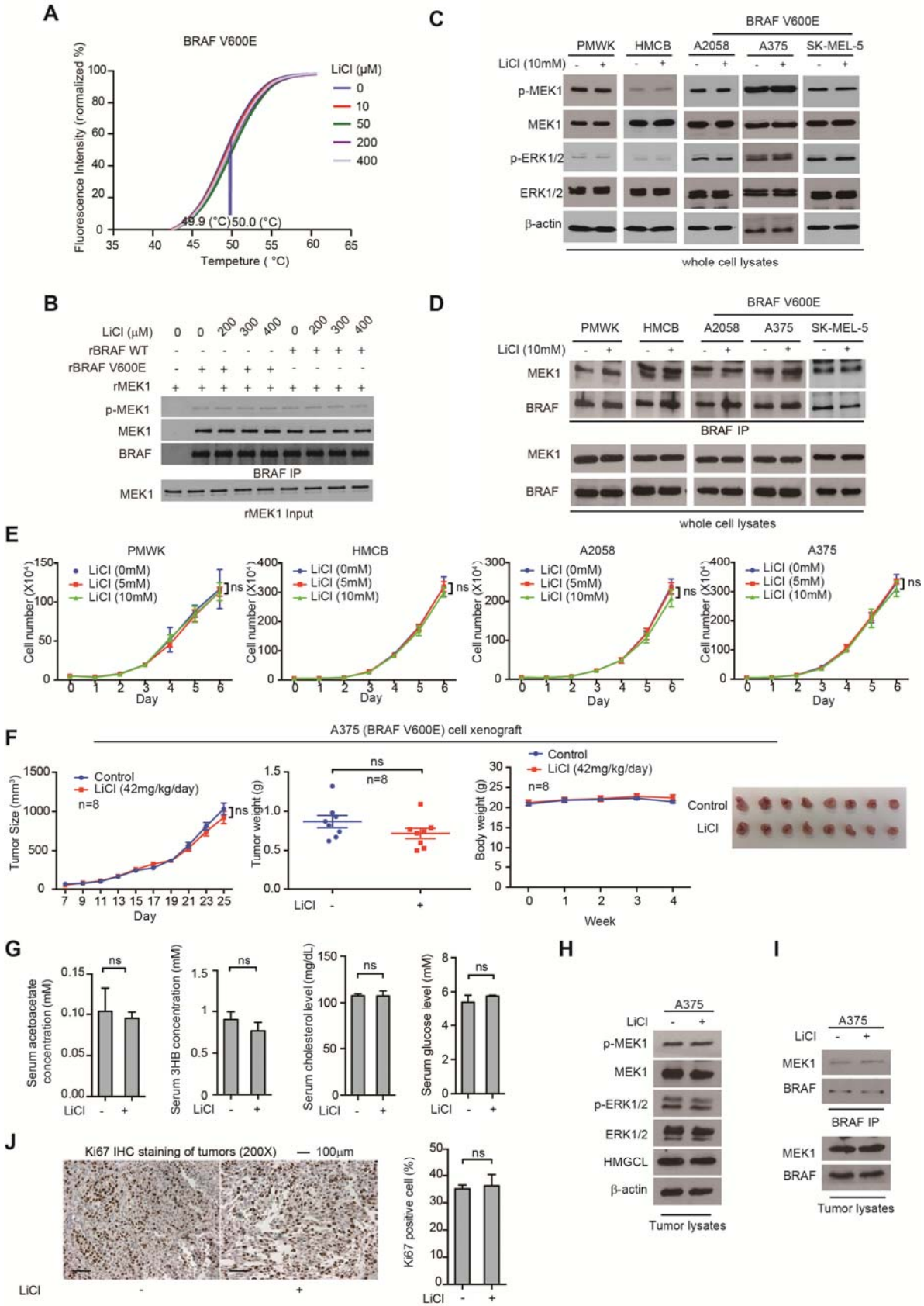

Figure S2. Lithium chloride has no effect on BRAF V600E-positive melanoma tumor growth. Related to Figure 2

(A) Thermal melt shift assay was performed to examine the BRAF V600E protein and lithium chloride interaction. Arrows indicate melting temperatures at 0 μM (*left*) and 400 μM (*right*).

(B) Effect of increasing concentrations of LiCl on rBRAF WT or rBRAF V600E binding to purified recombinant MEK1 (rMEK1).

(C-E) Effect of LiCl treatment on MEK1 and ERK1/2 phosphorylation (C), BRAF-MEK1 binding (D), and cell proliferation rates (E) in samples obtained from human melanoma PMWK, HMCB cells, or BRAF V600E positive melanoma A2058, A375, and/or SK-MEL-5 cells.

(F) Xenograft tumor growth and weight (*left* two panels) and size (*right* panel) in nude mice inoculated with human melanoma BRAF V600E-positive A375 cells and intraperitoneally injected with LiCl. Data are mean ± SEM for tumor growth and mean ± s.d. for tumor weight; p values were obtained by a two-way ANOVA test for tumor growth rates and a two-tailed Student's *t* test for tumor masses.

(G) AA, 3HB, cholesterol, and glucose levels in serum harvested from A375 xenograft mice intraperitoneally injected with LiCl. Data are mean ± s.d.; n=3; p values were obtained by a two-tailed Student's *t* test.

(H-I) Effect of LiCl treatment on MEK1 and ERK1/2 phosphorylation (H) and BRAF-MEK1 binding (I) in tumor samples from xenograft nude mice.

(J) Summarized results of immunohistochemical (IHC) staining assay. Representative images of IHC staining of Ki67 (brown color, *left*) and detection of Ki67-positive cells in tumor tissue samples (*right*) from A375 xenograft mice intraperitoneally injected with LiCl. Data are mean ± s.d.; p values were obtained by a two-tailed Student's *t* test.

Figure S3 related to Figure 2

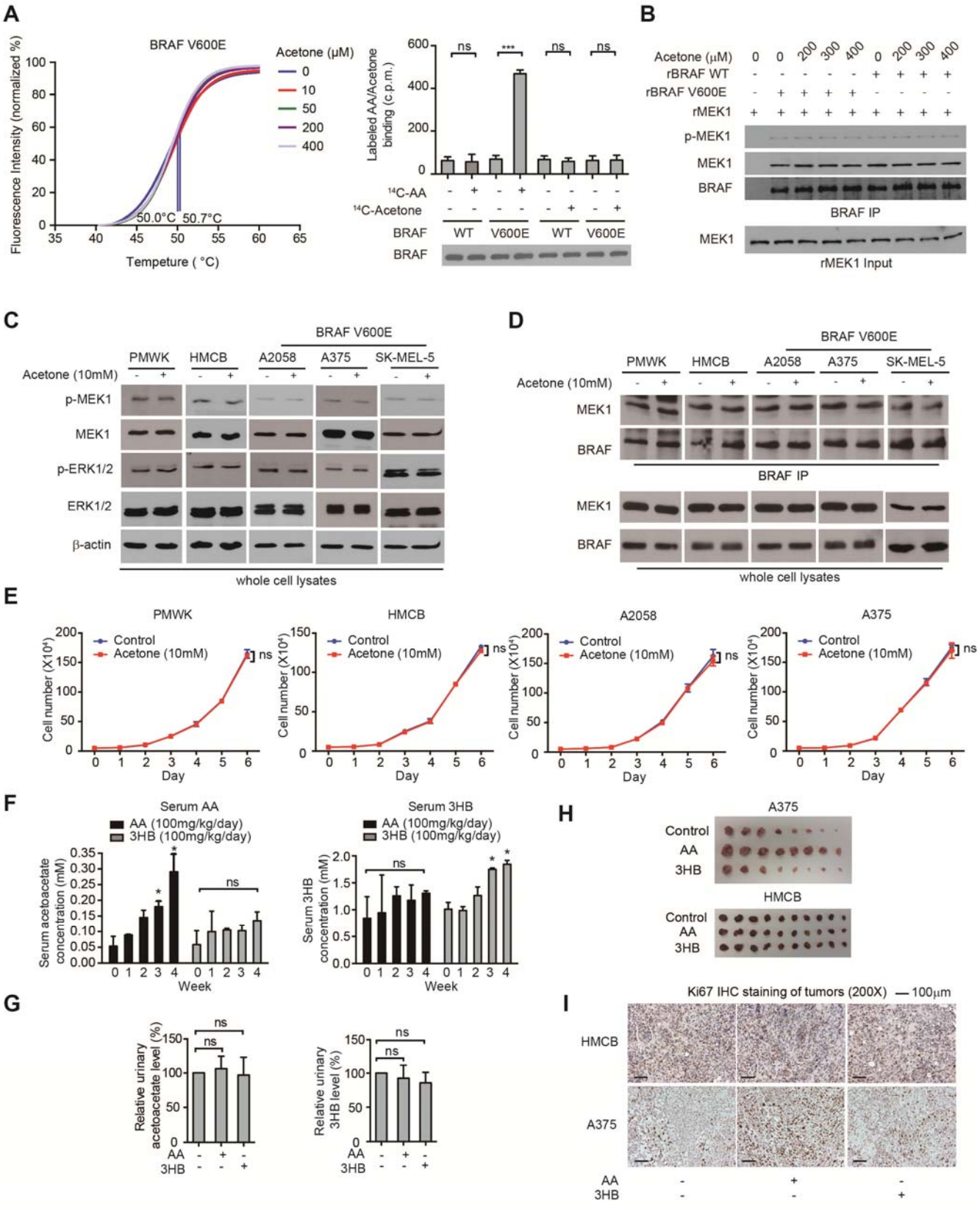

Figure S3. Acetone has no effect on BRAF V600E-positive melanoma cell proliferation. Related to Figure 2

(A) *Left panel*: Thermal melt shift assay was performed to examine the BRAF V600E protein and acetone interaction. Arrows indicate melting temperatures at 0 μM (*left*) and 400 μM (*right*). *Right panel*: results of a binding assay using purified BRAF wild type or V600E mutant proteins incubated with ^{14}C-labeled acetone.

(B) Effect of increasing concentrations of acetone on rBRAF WT or rBRAF V600E binding to purified recombinant MEK1 (rMEK1).

(C-E) Effect of acetone treatment on MEK1 and ERK1/2 phosphorylation (C), BRAF-MEK1 binding (D), and cell proliferation rates (E) in samples obtained from human melanoma PMWK, HMCB cells, or BRAF V600E positive melanoma A2058, A375, and/or SK-MEL-5 cells. Data are mean ± s.d.; n=3; p values were obtained by a two-tailed Student's *t* test.

(F) Weekly monitored AA (*left*) and 3HB (*right*) in serum harvested from nude mice that were intraperitoneally injected with AA or 3HB. Data are mean ± s.d.; n=3; p values were obtained by a two-tailed Student's *t* test.

(G) AA (*left*) and 3HB (*right*) levels in urine harvested from A375 xenograft mice that were intraperitoneally injected with AA or 3HB. Data are mean ± s.d.; n=3; p values were obtained by a two-tailed Student's *t* test.

(H) Xenograft tumor size in nude mice inoculated with A375 (*upper*) or HMCB (NRAS Q61K; *lower*) cells and intraperitoneally injected with AA or 3HB.

(I) Representative images of IHC staining of Ki67 (brown color) from xenograft mice. Scale bars represent 100 μM.

Figure S4 related to Figure 3

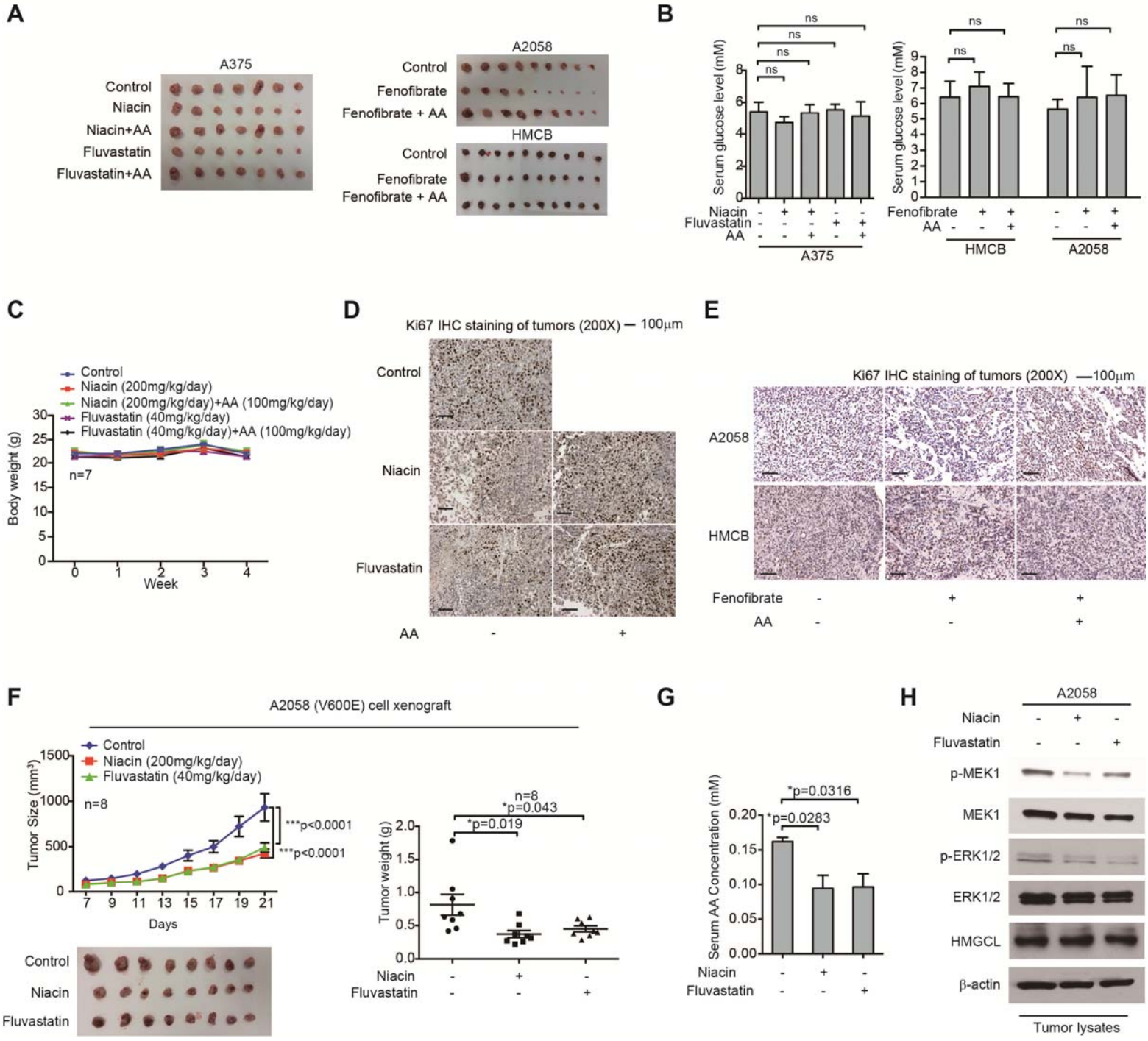

Figure S4. Lipid lowering agents decrease serum acetoacetate levels in xenograft mice and attenuate BRAF V600E-positive tumor growth. Related to Figure 3

(A) Xenograft tumor size in nude mice inoculated with human melanoma BRAF V600E-positive A375 cells (*left*) and orally treated with two different lipid lowering agents, niacin or fluvastatin, alone

or in combination with intraperitoneal injection with AA; and in mice inoculated with BRAF V600E-positive A2058 (*upper right*) or HMCB (NRAS Q61K, *lower right*) cells and orally treated with lipid lowering agent fenofibrate alone or in combination with intraperitoneal injection with AA.
(B-C) Glucose level in serum (B) and body weight (C) of xenograft nude mice in (A).
(D-E) Representative images of IHC staining of Ki67 (brown color) from xenograft mice treated with different lipid lowering agents alone or in combination with intraperitoneal injection with AA.
(F) Xenograft tumor growth (*upper left*), size (*lower left*) and weight (*right*) in nude mice inoculated with BRAF V600E-expressing A2058 cells and orally treated with lipid lowering agents including niacin or fluvastatin. Data are mean ± SEM for tumor growth and mean ± s.d. for tumor weight; *p* values were obtained by a two-way ANOVA test.
(G-H) AA level in serum (G) and MEK1 and ERK1/2 phosphorylation in tumor samples (H) from mice with A2058 xenografts that were orally treated with niacin or fluvastatin alone or in combination with intraperitoneal injection with AA. Data are mean ± s.d.; n=3; p values were obtained by a two-tailed Student's *t* test.

Figure S5 related to Figures 4 and 5

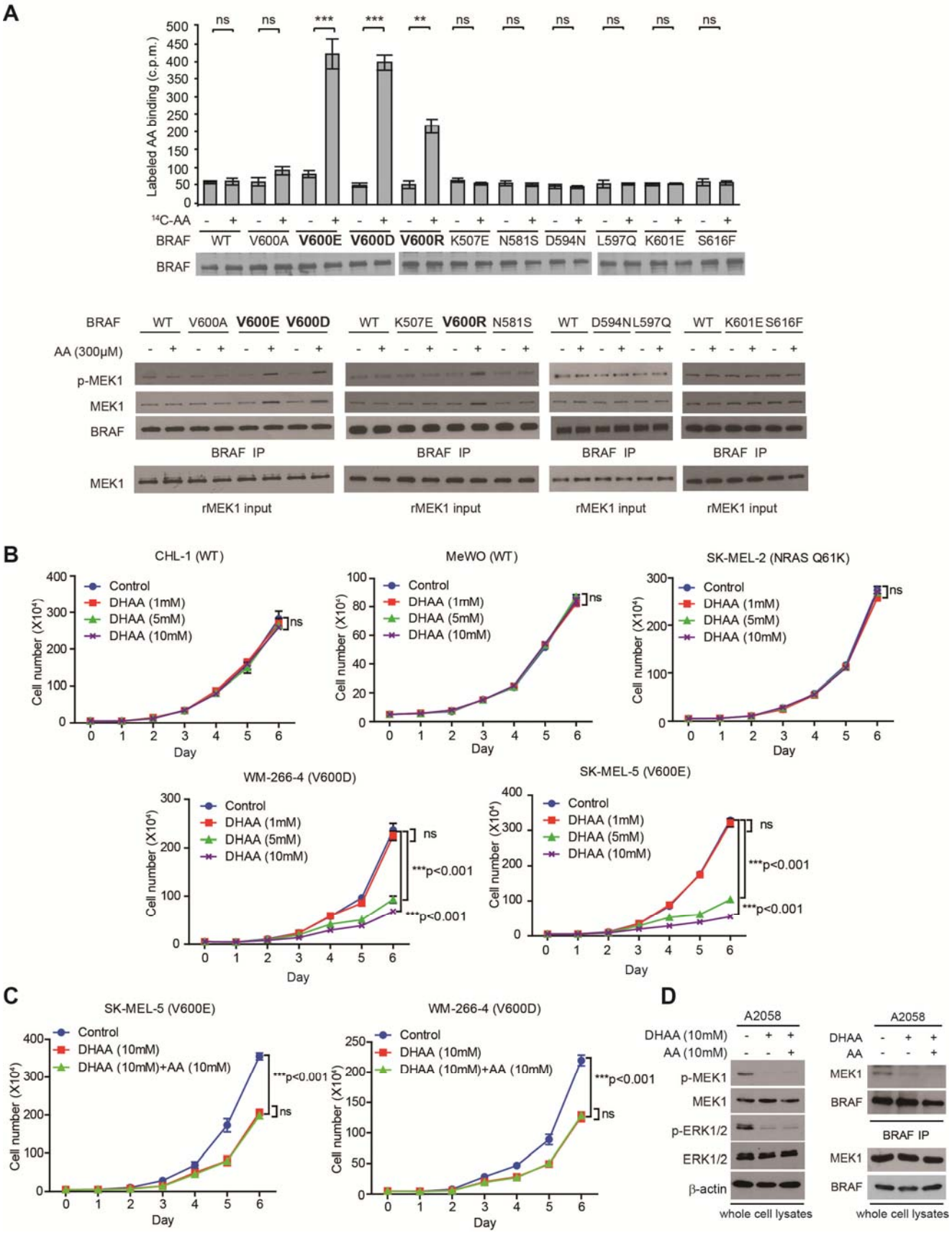

Figure S5. Acetoacetate selectively binds to and regulates BRAF V600D/E/R mutants. Related to Figure 4

(A) *Upper*: Radiometric metabolite-protein interaction analysis (*upper*) using ^{14}C-labeled acetoacetate incubated with diverse purified BRAF variants. *Lower*: BRAF-MEK1 binding and phosphorylation assays using acetoacetate (300 μM) incubated with immunoprecipitates of diverse BRAF mutants in the presence of purified recombinant MEK1 (rMEK1). Data are mean ± s.d.; n=3 each; *p* values were obtained by a two-tailed Student's *t* test.

(B) Effect of DHAA treatment on cell proliferation rates of diverse human melanoma cells. Cell proliferation rates were determined by daily cell counting. Data are mean ± s.d.; n=3; *p* values were obtained by a two-tailed Student's *t* test.

(C) Effect of DHAA with or without AA treatment on cell proliferation rates of BRAF-V600E positive human melanoma cells. Cell proliferation rates were determined by daily cell counting. Data are mean ± s.d.; n=3; *p* values were obtained by a two-tailed Student's *t* test.

(D) Effect of DHAA with or without AA treatment on MEK1 and ERK1/2 phosphorylation (*left*) and BRAF-MEK1 binding (*right*) in melanoma BRAF-V600E positive A2058 cells.

Figure S6 related to Figure 6

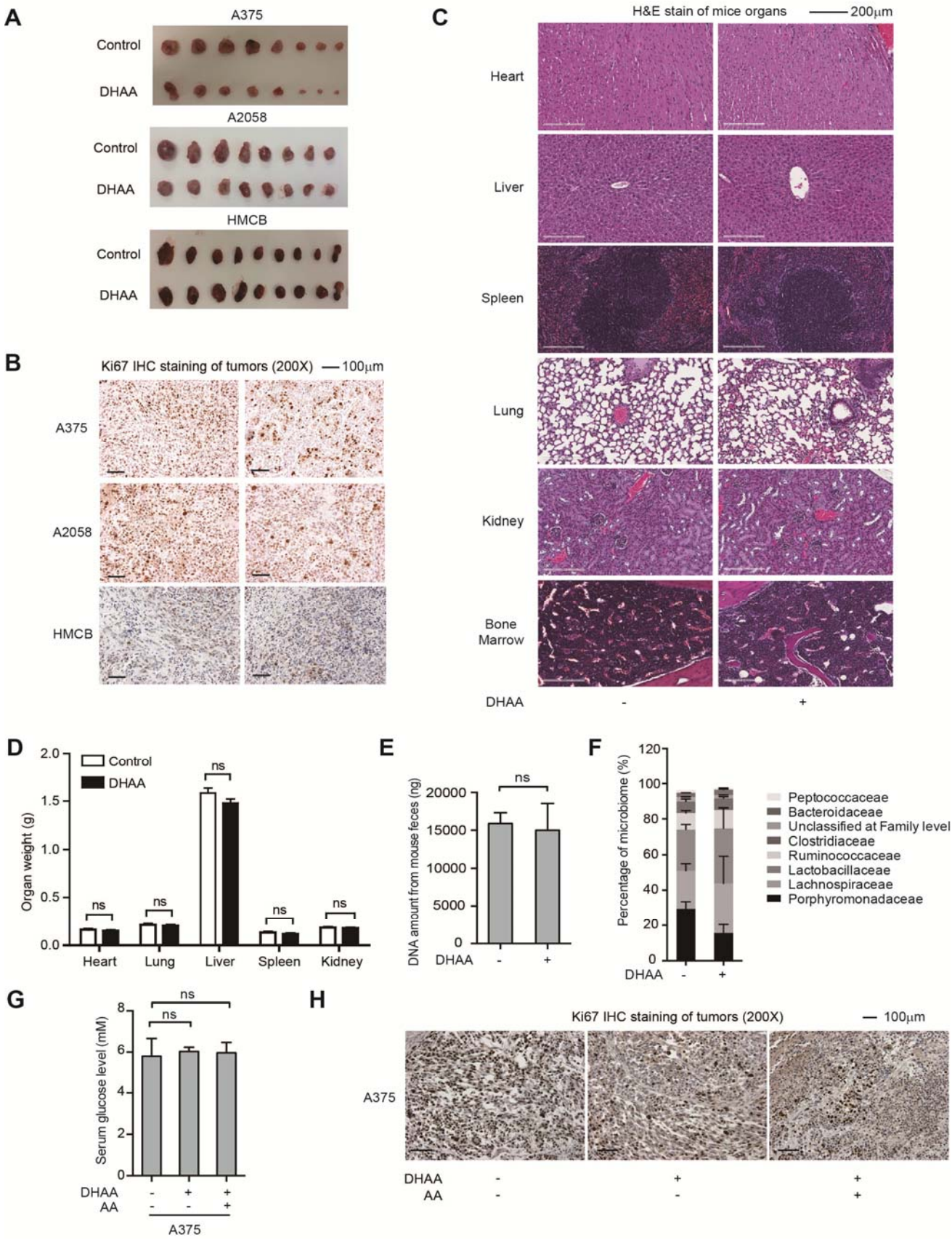

Figure S6. DHAA attenuates tumor growth potential of BRAF V600E-positive human melanoma cells. Related to Figure 6

(A) Xenograft tumor size in nude mice inoculated with human melanoma BRAF V600E-positive A375 (*upper*) or A2058 (*middle*) and HMCB (NRAS Q61K) (*bottom*) cells and intraperitoneally injected with DHAA.

(B) Representative images of IHC staining of Ki67 (brown color) in tumor samples from DHAA-treated xenograft mice. Scale bars represent 100 μM.

(C) Histological morphology of hematoxylin-eosin stained tissue sections of representative nude mice chronically treated with DHAA or water for ~4 weeks. Images were analyzed and captured using ImageScope software (Aperio Technologies Inc.) without any additional or subsequent image processing (20x). Scale bars represent 200 μM.

(D) Weight of diverse organs from nude mice chronically treated with DHAA or water for ~4 weeks.

(E) DNA amount extracted from ~100mg feces from DHAA-treated mice. Data are mean ± s.d.; n=2; *p* values were obtained by a two-tailed Student's *t* test.

(F) Gut microbiome components of DHAA-treated mice. Data are mean ± s.d.; n=2; *p* values were obtained by a two-tailed Student's *t* test.

(G) Glucose levels in serum obtained from A375 xenograft mice treated with DHAA with or without AA. Data are mean ± s.d.; n=3; *p* values were obtained by a two-tailed Student's *t* test.

(H) Representative images of IHC staining of Ki67 (brown color) from A375 xenograft mice treated with DHAA with or without AA. Scale bars represent 100 μM.

Figure S7 related to Figure 7

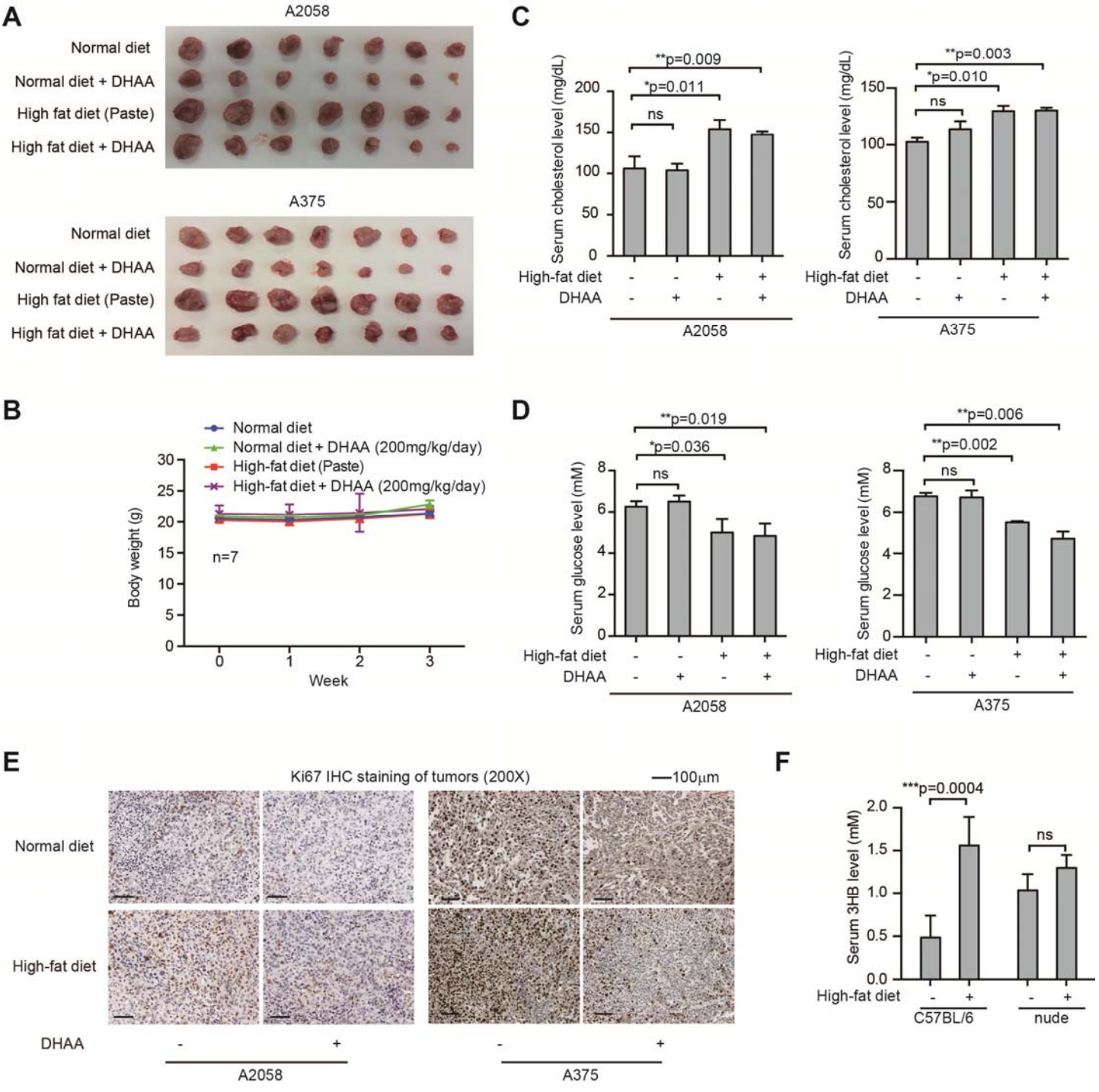

Figure S7. DHAA treatment reverses high-fat diet-enhanced BRAF V600E tumor growth in xenograft nude mice. Related to Figure 7

(A-B) Xenograft tumor size (A) and body weight (B) in nude mice inoculated with BRAF V600E-positive human melanoma A2058 (*upper*) and A375 (*lower*) cells and fed with normal or high-fat diets followed by intraperitoneal injection with DHAA.
(C-D) Cholesterol (C) and glucose (D) levels in serum harvested from xenograft mice. Data are mean ± s.d.; n=3; *p* values were obtained by a two-tailed Student's t test.
(E) Representative images of IHC staining of Ki67 (brown color) from xenograft mice. Scale bars represent 100 μM.
(F) Serum concentrations of 3HB in C57BL/6 mice and Balb/c nude mice treated with high-fat diet.

Table S1. CBC results of serum harvested from DHAA-treated A375 xenograft mice. Related to Figure 6

Test name	Normal range	Water	DHAA
RBC	6.5-10.1	9.47± 0.60	8.27± 2.27
MCV	42.3-55.9	50.45± 5.73	47.80± 0.42
HCT	32.8-48	48.00± 8.49	39.60± 11.17
MCH	13.7-18.1	16.70± 0.42	17.05± 0.07
MCHC	29.5-35.1	33.45± 4.60	35.65± 0.07
RDW%	0-99.9	16.75± 1.91	17.70± 0.57
RDWa	0-99.9	31.25± 2.19	30.55± 0.35
PLT	160-410	165.00± 33.94	220± 82.02
MPV	0-99.9	6.70± 0.14	6.75± 0.21
HGB	10-16.1	15.85± 0.64	14.10± 3.96
WBC	2.6-10.1	5.95± 0.35	7.50± 2.12
LYM	1.3-8.4	4.30± 0.42	5.9± 1.65
MONO	0-0.3	0.35± 0.07	0.4± 0.00
GRAN	0.4-2	1.30± 0.00	1.20± 0.57
LYM%	0-99.9	71.85± 2.47	78.75± 1.06
MONO%	0-99.9	5.85± 1.34	4.95± 1.20
GRAN%	0-99.9	22.3± 1.13	16.3± 2.26

EXTENDED EXPERIMENTAL PROCEDURES

Reagents. Acetoacetate (AA), 3-hydroxybutyric acid (3HB), dehydroacetic acid (DHAA), lithium chloride, actone, fenofibrate, niacin and fluvastatin were from Sigma-Aldrich. BRAF cDNA image clone were purchased from Open Biosystems. MEK1 cDNA image clone was from Addgene. Human BRAF was FLAG tagged by PCR and subcloned into pET53-derived or pLHCX-derived Gateway destination vector. Human BRAF was FLAG tagged by PCR and subcloned into pLHCX derived Gateway destination vector. The BRAF V600E mutant was generated using a site-directed mutagenesis kit as previously described (Kang et al., 2015). Mel-ST cells expressing BRAF WT, BRAF V600E and truncated BRAF (tBRAF) were generated as previously described (Kang et al., 2015) using retroviral vector pMSCV (Clontech) expressing FLAG-tagged BRAF variants. Antibodies against BRAF were from Santa Cruz Biotechnology. Antibodies against p-MEK1, MEK, p-ERK1/2, ERK1/2 and conformation specific mouse anti-rabbit IgG were from Cell Signaling Technology (CST). HMGCL and Ki67 antibodies were from Abcam. Antibody against β-actin was from Sigma-Aldrich.

Cell culture. PMWK, A2058, A375, WM-266-4, CHL-1, MeWo, SK-MEL-5 and MEL-ST cells were cultured in Dulbecco Modified Eagle Medium (DMEM) with 10% fetal bovine serum (FBS). HMCB and SK-MEL-2 cells were cultured in Eagle's Minimum Essential Medium (EMEM) with 10% FBS. All cells were cultured at 37°C and 5% CO_2.

Purification of BRAF variants and MEK1 proteins. $(His)_6$-tagged BRAF variants and MEK1 proteins were purified by sonication of high expressing BL21(DE3) pLysS cells obtained from a 250 mL culture subjected to IPTG-induction for 14 h at 30°C. Cell lysates were loaded onto a Ni-NTA column in 20 mM imidazole. After washing twice, the protein was eluted with 250 mM imidazole. Proteins were desalted on a PD-10 column and the purification efficiency was examined by Coomassie Blue staining and Western blot.

Cell proliferation. Cell proliferation assays were performed by daily counting of cell number. Briefly, 5×10^4 cells were seeded per well of a 6-well plate and cultured at 37°C in 5% CO_2. The indicated concentration of DHAA or AA was added into the culture media 4 h after first-day seeding. Culture media were changed every two days and fresh DHAA or AA was added. Cell number was recorded daily by trypan blue exclusion using a TC10 Automated Cell Counter (BioRad) or cell counting.

Immunoprecipitation. Cell or tumor lysates were incubated with anti-BRAF antibody overnight at 4°C. After incubation, protein G-Sepharose was used for precipitation. The beads were washed and eluted with SDS sample buffer for Western blotting analysis.

Thermal melt shift assay. The thermal melt shift assay was performed as previously described (Hitosugi et al., 2012). In brief, thermal shift assay of compound (DHAA)-protein (BRAF WT or BRAF V600E) interaction was performed in 96-well PCR plates with various compound

concentrations and 200 μg/ml protein in a buffer solution (20 mM Tris, 100 mM NaCl, pH 7.4). SYPRO orange was used as a dye to monitor the fluorescence change at 610 nm. DHAA was dissolved in double distilled water and added to the protein solution.

Cellular thermal melt shift assay. The cellular thermal shift assay was performed as previously described (Martinez Molina et al., 2013). Briefly, 293T cells were transfected with FLAG-BRAF-WT or V600E mutant. After 24 h, cells were collected, resuspended in TBS and lysed with three cycles of freeze-thaw using dry ice/ethanol slurry. The soluble fraction was separated by centrifugation at 18,000g for 20 min. The cell lysates were then incubated with vehicle control, AA (400 μM) or DHAA (400 μM) for 15 min at room temperature. Subsequently, the lysates were aliquoted into 9 PCR tubes and heated at 46, 49, 52, 55, 58, 61, 64, 67 and 70°C for 3 min. The precipitated proteins were removed by centrifugation at 18,000g for 20 min and the soluble proteins were subjected to Western blot analysis.

Radiometric ^{14}C-acetoacetate and BRAF binding assay. Purified recombinant BRAF protein variants were pre-bound with FLAG-beads, followed by incubating with the indicated concentrations of ^{14}C-labeled acetoacetate (American Radiolabeled Chemicals) in 1xTBS (50 mM Tris, 150 mM NaCl, pH 7.5) buffer for 4 h at 4°C. The appropriate amount of DHAA as previously described was then added into the reaction mixture to incubate for another 4 h at 4°C. Alternatively, bead-bound BRAF protein variants were incubated first with the indicated concentrations of DHAA in 1xTBS buffer for 4 h at 4°C, then the appropriate amount of ^{14}C-labeled acetoacetate as previously described was added into the reaction mixture to incubate for another 4 h at 4°C. The beads were then washed and bead-bound BRAF proteins were eluted by incubating with 10 μg 3xFLAG peptides (Sigma-Aldrich) for 1 h. Radioactive signals of BRAF-bound ^{14}C-labeled acetoacetate were detected by liquid scintillation counting.

Measurement of Vmax and Km of BRAF V600E. BRAF V600E activity towards ATP was determined as the rate of ATP consumption using the Kinase-Glo® luminescent kinase assay kit (Promega). Briefly, BRAF in vitro kinase assay was performed using purified BRAF V600E protein (100 ng) incubated with increasing concentrations of ATP and increasing concentrations of DHAA in the presence or absence of 300uM acetoacetate, using excessive amount of purified MEK1 as substrates. The luminescence was measured by plate reader (SPECTRA MAX, Molecular Devices) after the addition of Kinase-Glo® Reagent. The consumption rate of ATP was calculated and plotted using GraphPad Prism software.

Measurement of Kd for the binding of ^{14}C-acetoacetate to BRAF. The ^{14}C-acetoacetate-BRAF binding assay was performed by incubating bead-bound FLAG-BRAF variants with increasing amounts of ^{14}C-acetoacetate. The radioactivity of retained ^{14}C-acetoacetate on BRAF variants was detected by liquid scintillation counting. Kd values were calculated using GraphPad Prism Software.

Measurement of Ki of DHAA to BRAF in the presence of ^{14}C-acetoacetate. Bead-bound FLAG-BRAF variants were incubated with 300 μM ^{14}C-acetoacetate in TBS buffer for 4 h at 4°C, followed by further incubation with 0, 10, 20, 50, 100, 200, 500, 1000 μM DHAA for another 4 h at 4°C after unbound ^{14}C-acetoacetate was washed off. The bead-bound BRAF proteins were eluted with 10 μg FLAG peptides and the radioactivity of retained ^{14}C-acetoacetate on BRAF variants was detected by liquid scintillation counting. Ki values were calculated using GraphPad Prism Software.

Measurements of acetoacetate, 3HB, cholesterol, glucose and triglyceride. Acetoacetate levels in mouse serum and urine samples and tumor lysates were measured using the Acetoacetate Colorimetric Assay Kit (BioVision) following the manufacturer's instructions. In brief, serum, urine or tumor lysates were incubated with acetoacetate substrate at room temperature for 10 minutes. The alteration in absorbance (OD550) was measured in a kinetic mode. 3HB levels in mouse serum and urine samples were measured using the Ketone Body Assay Kit (Abnova) following the manufacturer's instructions. In brief, serum, urine or tumor lysates were incubated with cholesterol esterase, probe and enzyme mix provided in the kit for 60 minutes at 37 °C in dark. Alteration in absorbance at OD570 was measured. For cholesterol assay, total cholesterol levels in mouse serum samples were measured using the Total Cholesterol and Cholesteryl Ester Colorimetric/Fluorometric Assay Kit (Biovision) following the manufacturer's instructions. In brief, serum samples were incubated with cholesterol esterase, probe and enzyme mix provided in the kit for 60 minutes at 37 °C in dark. Alteration in absorbance at OD570 was measured. Glucose levels in mouse serum samples were measured using the Glucose Colorimetric/Fluorometric Assay Kit (Biovision) following the manufacturer's instructions. In brief, serum samples were incubated with glucose probe and enzyme mix provided in the kit for 30 minutes at 37 °C in dark. Alteration in absorbance at OD570 was measured. Triglyceride levels in mouse serum samples were measured using the Triglyceride Quantification Colorimetric/Fluorometric Kit (Biovision) following the manufacturer's instructions. In brief, serum samples were pre-incubated with lipase at room temperature for 20 minutes in dark. Then triglyceride probe and enzyme mix provided in the kit were added and incubated for 60 minutes at room temperature in dark. Alteration in absorbance at OD570 was measured.

BRAF and MEK1 binding assay. Recombinant BRAF variants and MEK1 were incubated in TBS buffer for 4 h at 4°C in the presence of 300μM AA, then increasing concentrations of DHAA were added and incubated for another 4h at 4°C, followed by incubation with anti-BRAF antibody overnight at 4°C. After incubation, protein G-Sepharose was used for precipitation. The beads were washed and eluted with SDS sample buffer for Western blotting analysis.

Animal models. The design and conduct of all experiments using mice was approved by the Institutional Animal Care and Use Committee of Emory University. For xenograft studies, nude mice (nu/nu, female 4-6-week-old, Harlan Laboratories) were subcutaneously injected with $1x10^6$ melanoma cells on the flank. Tumor growth was recorded every two days from one week after inoculation by measurement of two perpendicular diameters using the formula $4\pi/3$ x $(\text{width}/2)^2$ x (length/2). Mice were sacrificed ~4 weeks after inoculation. The masses of tumors (g) derived from

treatments were compared. Statistical analyses were performed by comparison in relation to the control group with a two-tailed paired Student's *t* test. Mice in the high-fat diet group started receiving paste high-fat diet (Bio serv F3666) or solid high-fat diet (Research Diets D12369B) one week before tumor cell inoculation and continued to receive the diet until the experimental endpoint. Mice in the control group received standard rodent diet (LabDiet 5015).

Caloric Profile (kcal/gm)

Food name	Normal	Paste High fat	Solid High fat
Company	LabDiet	Bio serv	Research Diets
Catalog	5015	F3666	D12369B
Protein	0.94 (19.8%)	0.34 (4.7%)	0.7 (10.4%)
Carbohydrate	1.24 (26.1%)	0.13 (1.8%)	0.007 (0.1%)
Fat	2.57 (54.1%)	6.76 (93.5%)	6.05 (89.5%)
Total	4.74 (100%)	7.24 (100%)	6.76 (100%)

The amount of solid high-fat diet and standard diet consumed by mice was recorded by weighing the food mass. Body weights of mice were recorded weekly. AA (100mg/kg/day), 3HB (100mg/kg/day), DHAA (200mg/kg/day) and LiCl (42mg/kg/day) were injected into mice intraperitoneally daily beginning on the day of tumor inoculation. Lipid lowering agents (fenofibrate (200mg/kg/day), niacin (200mg/kg/day), or fluvastatin (40mg/kg/day)) were given to mice by oral gavage beginning on the day of tumor inoculation and AA (100mg/kg/day) was intraperitoneally injected beginning on the same day. For gut microbiome analysis, nude mice were injected with DHAA (200mg/kg/day) for 4 weeks before feces collection. Feces from each mouse in the same cage were collected and mixed as one sample. ~100mg feces from each cage were sent to GENEWIZ company for 16S rRNA sequencing and gut microbiome analysis.

Immunohistochemical staining. Ki67 staining was performed as previously described (Kang et al., 2015). Resected tumors from xenograft mice were fixed in 10% buffered formalin, embedded in paraffin and mounted on slides. After deparaffinization and rehydration, mouse tumor sections were incubated in 3% hydrogen peroxide to suppress endogenous peroxidase activity. Antigen retrieval was achieved by microwaving the sections in 10mM sodium citrate (pH6.0). Sections were then blocked by incubation in 10% goat serum. Human Ki67 antibody (Abcam) was applied overnight at 4°C. Detection was achieved with the Dako IHC kit (Agilent technologies). Slides were stained with 3,3′-diaminobenzidine, washed, counterstained with hematoxylin, dehydrated, and mounted.

Histopathology and complete blood counts. Histopathology and complete blood counts were performed as previously described (Lin et al., 2015). For histopathological analysis, sections of mouse tissue were stained with hematoxylin and eosin and slides were digitally scanned at ×20 magnification using a ScanScope XT from Aperio Technologies. Images were analyzed and captured using ImageScope software (Aperio Technologies) without any additional or subsequent image processing. For complete blood counts, blood was collected retro-orbitally and immediately applied to a HemaVet 950FS (Drew Scientific) for generation of a complete hematology profile.

SUPPLEMENTAL REFERENCES

Hitosugi, T., Zhou, L., Elf, S., Fan, J., Kang, H.B., Seo, J.H., Shan, C., Dai, Q., Zhang, L., Xie, J., et al. (2012). Phosphoglycerate mutase 1 coordinates glycolysis and biosynthesis to promote tumor growth. Cancer Cell *22*, 585-600.

Kang, H.B., Fan, J., Lin, R., Elf, S., Ji, Q., Zhao, L., Jin, L., Seo, J.H., Shan, C., Arbiser, J.L., et al. (2015). Metabolic Rewiring by Oncogenic BRAF V600E Links Ketogenesis Pathway to BRAF-MEK1 Signaling. Mol Cell *59*, 345-358.

Lin, R., Elf, S., Shan, C., Kang, H.B., Ji, Q., Zhou, L., Hitosugi, T., Zhang, L., Zhang, S., Seo, J.H., et al. (2015). 6-Phosphogluconate dehydrogenase links oxidative PPP, lipogenesis and tumour growth by inhibiting LKB1-AMPK signalling. Nat Cell Biol *17*, 1484-1496.

Martinez Molina, D., Jafari, R., Ignatushchenko, M., Seki, T., Larsson, E.A., Dan, C., Sreekumar, L., Cao, Y., and Nordlund, P. (2013). Monitoring drug target engagement in cells and tissues using the cellular thermal shift assay. Science *341*, 84-87.